Spin-Crossover-Triggered Linkage Isomerization by the Pedal-like Motion of the Azobenzene Ligand in a Neutral Heteroleptic Iron(III) Complex

Miyawaki, Atsuhiro ; Eda, Kazuo ; Mochida, Tomoyuki ; Sakurai, Takahiro ; Ohta, Hitoshi ; Nakajima, Takahito ; Takahashi, Kazuyuki

(Citation)
Inorganic Chemistry,60(17):12735-12739

(Issue Date)
2021-09-06

(Resource Type)
journal article

(Version)
Accepted Manuscript

Spin-Crossover Triggered Linkage Isomerization by the Pedal-like Motion of the Azobenzene Ligand in a Neutral Heteroleptic Iron(III) Complex

Atsuhiro Miyawaki,[†] Kazuo Eda,[†] Tomoyuki Mochida,[†,‡] Takahiro Sakurai,[§] Hitoshi Ohta,[¶] Takahito Nakajima,[‖,†] Kazuyuki Takahashi*[,†]

[†] Department of Chemistry, Graduate School of Science, Kobe University, 1-1 Rokkodai-cho, Nada-ku, Kobe, Hyogo 657-8501, Japan. E-mail: ktaka@crystal.kobe-u.ac.jp

[‡] Research Center for Membrane and Film Technology, Kobe University, 1-1 Rokkodai-cho, Nada-ku, Kobe, Hyogo 657-8501, Japan

[§] Research Facility Center for Science and Technology, Kobe University, 1-1 Rokkodai-cho, Nada-ku, Kobe, Hyogo 657-8501, Japan

[¶] Molecular Photoscience Research Center, Kobe University, 1-1 Rokkodai-cho, Nada-ku, Kobe, Hyogo 657-8501, Japan

[‖] Computational Molecular Science Research Team, RIKEN Center for Computational Science, 7-1-26 Minatojima-minamimachi, Chuo-ku, Kobe, Hyogo 650-0047, Japan

Supporting Information Placeholder

ABSTRACT: The temperature dependence of magnetic susceptibility of $[Fe^{III}(azp)(qsal\text{-}Me)]\cdot 0.5CH_3OH$ [Hqsal-Me = 5-methyl-*N*-(8-quinoyl)salicylaldimine, H_2azp = 2,2'-azobisphenol] demonstrated that the spin-crossover (SCO) transition behavior changed from an abrupt transition to consecutive gradual conversions, and moreover, the initial abrupt transition was recovered keeping the complex at room temperature. The variable temperature crystal structures revealed that an SCO triggered linkage isomerization of the azobenzene ligand from one orientation to two disordered orientations and the relaxation from the disordered orientations to the original orientation occurred. The high-spin to low-spin relaxation kinetics and theoretical calculation indicate that the pedal-like motion of the azobenzene ligand can be on in the high-spin state, whereas off in the low-spin state.

A molecular switch has attracted a great deal of attention in chemical and materials science fields. The photoinduced *cis-trans* isomerization of azobenzene derivatives[1] and ring formation-dissociation reaction of diarylethene derivatives[2] are well-known molecular photo-switching phenomena that can control not only the electronic- and spin-states of a molecule but also the mechanical motion of bulk materials such as blended polymers and single crystals. Spin crossover (SCO) between the low-spin (LS) and high-spin (HS) states in a transition metal coordination complex is one of the molecular switching phenomena that accompany the change in a spin-state and molecular structure induced by various external stimuli such as temperature, pressure, and light.[3,4] Much attention has been paid to the applications of SCO complexes as a molecular switch to control other functions such as electrical conductivity,[5–8] magnetic,[9–12] dielectric,[13,14] and optical properties.[15–17] We herein report the observation that SCO can control the pedal-like molecular motion of a coordination azobenzene ligand.

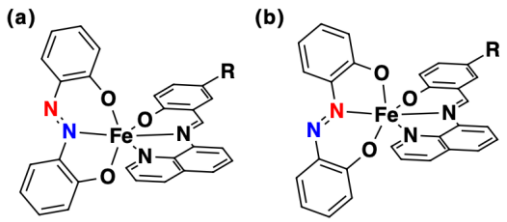

Figure 1. Two possible linkage isomers of the heteroleptic [Fe(azp)(qsal-R)] molecule in **1** (R = H) and **2** (R = CH_3). (a) The original (OR) linkage isomer determined in a pristine crystal of **2**. (b) The opposite (OP) linkage isomer.

2,2'-azobisphenol (H_2azp) is one of the azo dyes that can be utilized as an intense coloring reagent to metal ions. Recently we discovered the deprotonated azp dianion molecule afforded various Fe(III) SCO complexes in either homoleptic anionic form[18,19] or heteroleptic neutral form,[20,21] where the azp molecule was bound to the Fe(III) ion as a tridentate *O,N,O*-coordination ligand.

Since both nitrogen atoms in the azo group can coordinate to a central metal ion, the azp ligand in the heteroleptic complexes may give two possible linkage isomers (Figure 1). The orientational disorder of the azp ligand was sometimes reported due to the existence of linkage isomers in the complexes.[18,22]

Among the heteroleptic azp complexes, [Fe(azp)(qsal-H)]·0.5CH_3OH (**1**) exhibited an abrupt SCO transition with a thermal hysteresis [Hqsal-H = *N*-(8-quinoyl)salicylaldimine].[20] To investigate the substitution effect on the SCO behavior, the methyl derivative [Fe(azp)(qsal-Me)]·0.5CH_3OH (**2**) was synthesized and characterized [Hqsal-Me = 5-methyl-*N*-(8-quinoyl)salicylaldimine]. We found the SCO transition from the LS to HS states in **2** induced the azp ligand linkage isomerization from one orientation to dynamically disordered orientations between the original (OR) and opposite (OP) linkage isomers (Figure 1). Moreover, the relaxation from the OP isomer to the OR isomer was unexpectedly observed even at room temperature. The relaxation kinetics and computational analyses revealed that the pedal-like motion of the azp ligand molecule can be on in the HS state, whereas the motion may be off in the LS state. Therefore, the spin-state change of a metal center can switch the ligand motion in **2**.

The heteroleptic complex **2** was synthesized by the ligand exchange reaction between the corresponding homoleptic cationic and anionic[18] complexes in methanol solutions according to a modified procedure in the literature.[20] The composition of **2** was confirmed by microanalysis and single-crystal X-ray structural analysis.

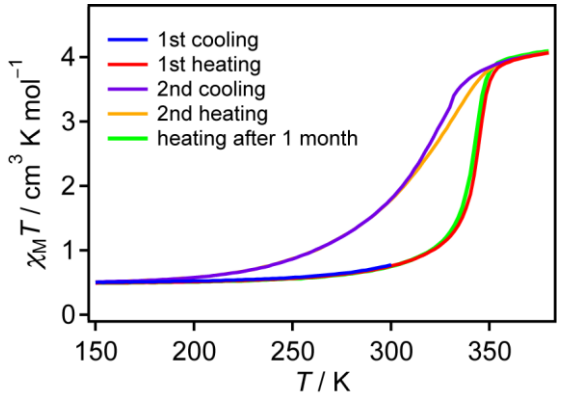

Figure 2. Temperature dependence of the $\chi_M T$ products for **2** in the temperature range of 150–380 K at a scan rate of 2 K min^{-1}.

The temperature variations of magnetic susceptibility for **2** are shown in Figure 2. The $\chi_M T$ value of a pristine sample was 0.78 cm^3 K mol^{-1} at 300 K, suggesting that **2** was almost in the LS state. On decreasing temperatures, the $\chi_M T$ values decreased gradually down to 250 K and then were almost constant. The $\chi_M T$ value of the pristine sample was 0.46 cm^3 K mol^{-1} at 10 K. On heating the sample, the $\chi_M T$ values followed the initial cooling trace and then increased abruptly at around 310 K, indicating the SCO transition to the HS state took place ($T_{1/2}\uparrow$ = 340 K). The $\chi_M T$ values reached 4.07 cm^3 K mol^{-1} at 380 K. On consecutive cooling, the $\chi_M T$ values started to decrease at 350 K and a more gradual conversion occurred and completed at 190 K ($T_{1/2}\downarrow$ = 302 K). Further consecutive heating the $\chi_M T$ values followed the gradual conversion trace up to 300 K and then a small thermal hysteresis was observed ($T_{1/2}\uparrow$ = 302 K). The gradual conversion was reproducible at a cooling and heating speed of 2 K min^{-1}. Therefore, the temperature variations of the $\chi_M T$ products were dramatically changed after the sample experienced the initial SCO transition. Very interestingly when we measured the magnetic susceptibility of the SCO-experienced sample kept at room temperature for one month, the initial abrupt SCO transition that the pristine sample exhibited was recovered. The recovery of the magnetic susceptibility after aging at room temperature was reproducible (Figure S1). This observation suggested that complex **2** that showed the gradual conversion may be in a thermally quenched state.

To clarify the thermal stability of **2**, the thermogravimetry analysis was carried out. The loss of solvated methanol molecules began above 450 K (Figure S2). Thus, this unusual magnetic behavior did not originate from either elimination or exchange of solvate methanol molecules. The differential scanning calorimetry (DSC) analysis of **2** was performed at a scan speed of 10 K min^{-1} (Figure S3 and Table S1). On heating a pristine sample from 273 to 400 K, a sharp endothermic peak appeared at 337 K. On consecutive cooling to 123 K, a broad exothermic peak was observed at 320 K. On further heating the sample to 400 K again, the DSC curve consisted of only a broad endothermic peak. The difference between the initial and second heating DSC curves was in good agreement with that in the $\chi_M T$ product between the initial and second heating scans.

To clarify the origin of this unusual thermal-magnetic behavior, variable-temperature single-crystal X-ray analyses were performed on one single crystal in the following order: pristine crystal at 90 K (**2-pr**), SCO-experienced crystal at 423 K (**2-ex**), thermally quenched crystal at 90 K (**2-qu**), and one-month-aged crystal at 90 K (**2-ag**). The crystallographic data are listed in Table S2. All the crystals belong to the triclinic system with *P*-1 and are isostructural to the parent complex **1**. The asymmetric unit contained one [Fe(azp)(qsal-Me)] molecule and a half methanol molecule. Both divalent azp anion and monovalent qsal-Me anion were coordinated to a Fe^{III} ion as tridentate ligands in an almost perpendicular manner, to construct a pseudo-octahedral FeN_3O_3 coordination sphere (Figures 3 and S4). The coordination bond lengths and distortion parameters are listed in Table S3. The comparison with these parameters of the parent complex[20] revealed that **2-pr**, **2-qu**, and **2-ag** were in the LS state, whereas **2-ex** was in the HS state.

Therefore, the initial spin transition from **2-pr** to **2-ex** originated from the SCO transition. It should be noted that the azp ligands in **2-pr** and **2-ag** were ordered**,** whereas in **2-ex** and **2-qu** were disordered. The change from the ordered ligand orientation in **2-pr** to the disordered ones in **2-ex** indicates that the linkage isomerization should take place after the initial SCO transition. Moreover, the disordered ligand orientations in **2-qu** suggest that the ligand orientations may be frozen at a cooling speed of several K min^{-1}. On the other hand, the recovery to the OR orientation in **2-ag** implies that the reverse transformation from the OP to OR isomers may occur even at room temperature.

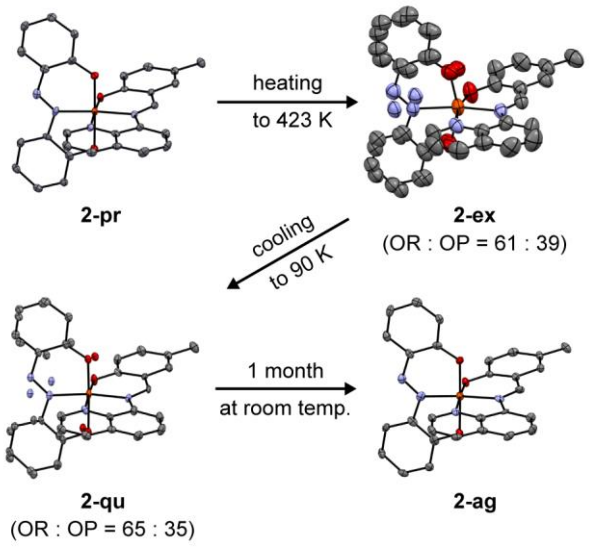

Figure 3. ORTEP drawings with a 50% probability of the molecular structures of **2** at consecutive thermal treatments. The ratios in the parenthesis are the ratios of the original (OR) to the opposite (OP) orientations. The atoms of the OP isomer are depicted without bonding lines.

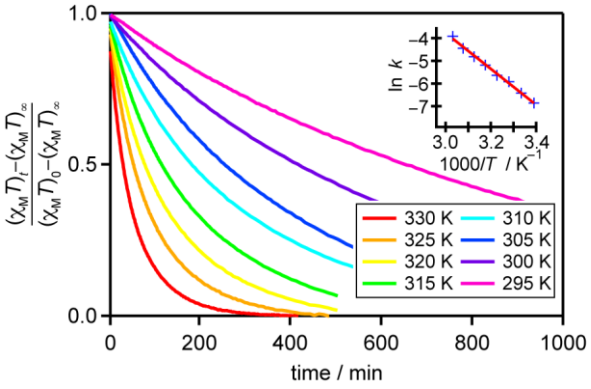

Figure 4. Time-dependent magnetic relaxation from the HS to LS states at various temperatures. Inset indicates the Arrhenius plot from the rate constants obtained by the JMAK model, where the red line shows the best-fitted one.

To gain an insight into the relaxation kinetics from the HS to LS states, the time-dependent magnetic susceptibility was monitored at various constant temperatures. The relaxation curves from the residual HS to LS states at all setting temperatures are depicted in Figure 4. The relaxation curves in the solid-state can be fitted with a modified Johnson, Mehl, Avrami, and Kolmogorov (JMAK) model.[23]

$$(\chi_M T)_t = (\chi_M T)_\infty + \{(\chi_M T)_0 - (\chi_M T)_\infty\}\exp\left[-(k\cdot t)^n\right] \quad \cdots \text{ eq. 1}$$

where $(\chi_M T)_0$ is the $\chi_M T$ value at the beginning of the measurement t = 0 and $(\chi_M T)_\infty$ is the asymptotic $\chi_M T$ value for infinity time $t = \infty$, k is the transformation rate constant, and n is the Avrami exponent. The fitted parameters are listed in Table S4. Since the value of the Avrami exponent n minus 1 relates the dimensionality of the nucleation of the LS state, the Avrami exponents of around 1 indicated that the HS-to-LS relaxation occurred almost independently in **2**. An Arrhenius plot of ln k vs. $1/T$ gave an almost linear relationship with an activation energy of 65.8(16) kJ mol^{-1} (Figure 4 inset). Therefore, the relaxation from the residual HS to LS states may be a single process. The activation energy was comparable to those of the linkage isomerism of sodium nitroprusside[24,25] or the pedal-like motion of stilbene derivatives,[26] and moreover, the azobenzene derivatives were known to exhibit the pedal-like motion on heating.[27] Therefore, we can assume that the pedal-like motion of the azp ligand may be related to the relaxation in **2**.

To compute the activation energies of the pedal-like motion of the azp ligand for the LS and HS states, the molecular geometries of the transition state (TS) in a gas phase were explored using the Gaussian 16 program package[28] at the B3LYP* functional[29] by the synchronous transit-guided quasi-Newton (STQN) method[30] with the QST3 option. The initial geometry of TS for the QST3 exploration was obtained by the nudged elastic band (NEB) method[31] using the NTChem program.[32] The thermochemistry parameters are listed in Table S5 and the schematic energy diagram is depicted in Figure 5. The optimized TS structures for the LS and HS states were similar to each other, where the azo group of the azp ligand was bound to the Fe(III) ion in an η^2 manner (Figure 5). The intrinsic reaction coordinate (IRC) calculations[33] for the TS structures in the LS and HS states revealed that the TS structures arise from the pedal-like motion of the azp ligand (Supporting information). The Gibbs energy differences of the OR and OP isomers to TS in the HS state at 298 K were 92.0 and 90.5 kJ mol^{-1}, respectively, whereas those in the LS state were the same value of 197.0 kJ mol^{-1}. These energy differences suggest that the pedal-like motion of the azp ligand can take place only when the complex is in the HS state. To obtain the Gibbs energy of activation for the relaxation of magnetic susceptibility, we applied the Eyring equation to the parameters given by the JMAK model. The enthalpy and entropy differences of activation are 63.2(16) kJ mol^{-1} and −87.5(5) J mol^{-1} K^{-1}, respectively (Figure S5). The Gibbs energy difference of activation at

298.15 K is 89.1(18) kJ mol^{-1}, which is in good agreement with the Gibbs energy difference computated in the HS state. These results strongly indicate that the residual HS spin state of the Fe(III) ion may be closely coupled to the pedal-like motion of the azp ligand. The absence of orientational disorder of the azp ligand of the pristine LS complex and the unidirectional relaxation to the OR orientational isomer suggest that the pedal-like motion of the azp ligand may be on in the HS state, whereas off in the LS state. Similar spin-state-dependent pyrazine ligand rotation in an SCO metal-organic framework was recently reported.[34] These spin-state-dependent ligand motions arise from the weakness of Fe-N coordination bonds due to the occupancy of e_g-type antibonding orbitals in the HS state.

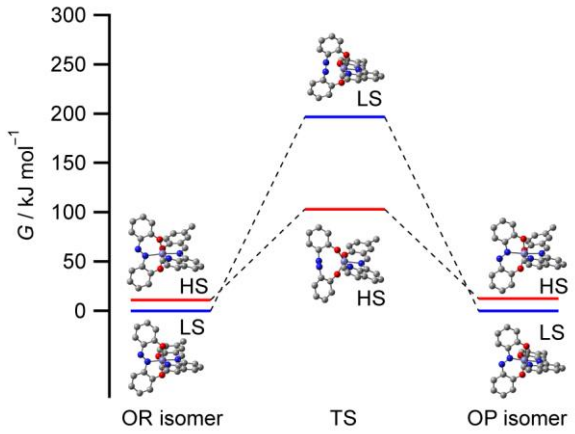

Figure 5. Energy diagram of the [Fe(azp)(qsal-Me)] molecules optimized at the B3LYP* functional in a gas phase at 298 K. The Gibbs energy of the LS isomer is set to zero.

In summary, we demonstrated the synthesis, crystal structures, physical measurements, and theoretical calculations of the methyl-substituted neutral heteroleptic Fe(III) complex **2** from the azobenzene ligand. The ligand orientational disorder, the HS-to-LS relaxation, and computed TS energies revealed that the SCO transition from the LS to HS state would be coupled to the pedal-like motion of the azobenzene ligand, resulting in linkage isomerization in complex **2**. This SCO-induced linkage isomerization indicates that the spin-state of a transition metal complex can switch not only the molecular motion of a coordinated ligand but also the bonding and dissociation of a coordination bond. The former leads to the possibility of the on-off switch of motion for molecular machines and actuators, the latter may lead to the elucidation of a chemical reaction mechanism involved in metal complex catalysts and bioinorganic molecular functional systems having potential SCO metal centers. Further investigations from the point of view of intermolecular interactions are needed to clarify the mechanisms of the unidirectional relaxation to the OR isomer and the change in SCO transition.

ASSOCIATED CONTENT

Supporting Information.

The Supporting Information is available free of charge on the ACS Publications website.

Synthesis, physical measurement details, and computational calculation methods, including Figures S1–S5 and Tables S1–S7 (PDF)
Crystal Structures for **2-pr**, **2-ex**, **2-qu**, and **2-ag** (CIF)
Pedal-like motion movie in the high-spin state (MP4)

AUTHOR INFORMATION

Corresponding Author

* ktaka@crystal.kobe-u.ac.jp

ACKNOWLEDGMENT

K. T. is grateful to Prof. Yoshihito Shiota at Kyushu University for discussion about theoretical calculations and Kenji Yoza in Bruker Japan Corporation for assistance with data processing on the crystal structure analysis. This work was partially supported by a Grant-in-Aid for Scientific Research (C) (No. 19K05402) from the Ministry of Education, Culture, Sports, Science, and Technology of Japan, and a grant from CASIO foundation. This work was carried out by the joint research program of Molecular Photoscience Research Center, Kobe University. A part of the computations were performed at the Research Center for Computational Science, Okazaki, Japan.

REFERENCES

(1) Yamada, M.; Kondo, M.; Mamiya, J.; Yu, Y.; Kinoshita, M.; Barrett, C. J.; Ikeda, T. Photomobile Polymer Materials: Towards Light-Driven Plastic Motors. *Angew. Chemie Int. Ed.* **2008**, *47*, 4986–4988.
(2) Irie, M.; Fukaminato, T.; Matsuda, K.; Kobatake, S. Photochromism of Diarylethene Molecules and Crystals: Memories, Switches, and Actuators. *Chem. Rev.* **2014**, *114*, 12174–12277.
(3) *Spin Crossover in Transition Metal Compounds I–III*; Gütlich, P.; Goodwin, H. A., Eds.; Topics in Current Chemistry; Springer: Berlin/Heidelberg, Germany, 2004.
(4) *Spin-Crossover Materials*; Halcrow, M. A., Ed.; John Wiley & Sons, Ltd.: Oxford, UK, 2013.
(5) Takahashi, K.; Cui, H.-B.; Okano, Y.; Kobayashi, H.; Einaga, Y.; Sato, O. Electrical Conductivity Modulation Coupled to a High-Spin−Low-Spin Conversion in the Molecular System [Fe^{III}(qsal)$_2$][Ni(dmit)$_2$]$_3$·CH$_3$CN·H$_2$O. *Inorg. Chem.* **2006**, *45*, 5739–5741.
(6) Takahashi, K.; Cui, H.-B.; Okano, Y.; Kobayashi, H.; Mori, H.; Tajima, H.; Einaga, Y.; Sato, O. Evidence of the Chemical Uniaxial Strain Effect on Electrical Conductivity in the Spin-Crossover Conducting Molecular System: [Fe^{III}(qnal)$_2$][Pd(dmit)$_2$]$_5$·Acetone. *J. Am. Chem. Soc.* **2008**, *130*, 6688–6689.
(7) Phan, H.; Benjamin, S. M.; Steven, E.; Brooks, J. S.; Shatruk, M. Photomagnetic Response in Highly Conductive Iron(II) Spin-Crossover Complexes with TCNQ Radicals. *Angew. Chem. Int. Ed.* **2015**, *54*, 823–827.
(8) Ishikawa, R.; Ueno, S.; Nifuku, S.; Horii, Y.; Iguchi, H.; Miyazaki, Y.; Nakano, M.; Hayami, S.; Kumagai, S.; Katoh, K.; et al. Simultaneous Spin-Crossover Transition and Conductivity Switching in a Dinuclear Iron(II) Coordination Compound Based on 7,7′,8,8′-Tetracyano-p-Quinodimethane. *Chem. - A Eur. J.* **2020**, *26*, 1278–1285.
(9) Nihei, M.; Tahira, H.; Takahashi, N.; Otake, Y.; Yamamura, Y.; Saito, K.; Oshio, H. Multiple Bistability and Tristability with Dual

Spin-State Conversions in $[Fe(dpp)_2][Ni(mnt)_2]_2 \cdot MeNO_2$. *J. Am. Chem. Soc.* **2010**, *132*, 3553–3560.
(10) Ohkoshi, S.; Imoto, K.; Tsunobuchi, Y.; Takano, S.; Tokoro, H. Light-Induced Spin-Crossover Magnet. *Nat. Chem.* **2011**, *3*, 564–569.
(11) Ababei, R.; Pichon, C.; Roubeau, O.; Li, Y.-G.; Bréfuel, N.; Buisson, L.; Guionneau, P.; Mathonière, C.; Clérac, R. Rational Design of a Photomagnetic Chain: Bridging Single-Molecule Magnets with a Spin-Crossover Complex. *J. Am. Chem. Soc.* **2013**, *135*, 14840–14853.
(12) Fukuroi, K.; Takahashi, K.; Mochida, T.; Sakurai, T.; Ohta, H.; Yamamoto, T.; Einaga, Y.; Mori, H. Synergistic Spin Transition between Spin Crossover and Spin-Peierls-like Singlet Formation in the Halogen-Bonded Molecular Hybrid System: $[Fe(Iqsal)_2][Ni(dmit)_2] \cdot CH_3CN \cdot H_2O$. *Angew. Chem. Int. Ed.* **2014**, *53*, 1983–1986.
(13) Jornet-Mollá, V.; Duan, Y.; Giménez-Saiz, C.; Tang, Y.-Y. Y.; Li, P.-F. F.; Romero, F. M.; Xiong, R.-G. G. A Ferroelectric Iron(II) Spin Crossover Material. *Angew. Chem. Int. Ed.* **2017**, *56*, 14052–14056.
(14) Akiyoshi, R.; Hirota, Y.; Kosumi, D.; Tsutsumi, M.; Nakamura, M.; Lindoy, L. F.; Hayami, S. Ferroelectric Metallomesogens Composed of Achiral Spin Crossover Molecules. *Chem. Sci.* **2019**, *10*, 5843–5848.
(15) Ohkoshi, S. I.; Takano, S.; Imoto, K.; Yoshikiyo, M.; Namai, A.; Tokoro, H. 90-Degree Optical Switching of Output Second-Harmonic Light in Chiral Photomagnet. *Nat. Photonics* **2014**, *8*, 65–71.
(16) Lochenie, C.; Schötz, K.; Panzer, F.; Kurz, H.; Maier, B.; Puchtler, F.; Agarwal, S.; Köhler, A.; Weber, B. Spin-Crossover Iron(II) Coordination Polymer with Fluorescent Properties: Correlation between Emission Properties and Spin State. *J. Am. Chem. Soc.* **2018**, *140*, 700–709.
(17) Wang, C.-F.; Yang, G.-Y.; Yao, Z.-S.; Tao, J. Monitoring the Spin States of Ferrous Ions by Fluorescence Spectroscopy in Spin-Crossover-Fluorescent Hybrid Materials. *Chem. - A Eur. J.* **2018**, *24*, 3218–3224.
(18) Takahashi, K.; Kawamukai, K.; Okai, M.; Mochida, T.; Sakurai, T.; Ohta, H.; Yamamoto, T.; Einaga, Y.; Shiota, Y.; Yoshizawa, K. A New Family of Anionic Fe^{III} Spin Crossover Complexes Featuring a Weak-Field N_2O_4 Coordination Octahedron. *Chem. Eur. J.* **2016**, *22*, 1253–1257.
(19) Murata, S.; Takahashi, K.; Sakurai, T.; Ohta, H.; Yamamoto, T.; Einaga, Y.; Shiota, Y.; Yoshizawa, K. The Role of Coulomb Interactions for Spin Crossover Behaviors and Crystal Structural Transformation in Novel Anionic Fe(III) Complexes from a π-Extended ONO Ligand. *Crystals* **2016**, *6*, 49.
(20) Murata, S.; Takahashi, K.; Mochida, T.; Sakurai, T.; Ohta, H.; Yamamoto, T.; Einaga, Y. Cooperative Spin-Crossover Transition from Three-Dimensional Purely π-Stacking Interactions in a Neutral Heteroleptic Azobisphenolate Fe^{III} Complex with a N_3O_3 Coordination Sphere. *Dalton Trans.* **2017**, *46*, 5786–5789.
(21) Miyawaki, A.; Mochida, T.; Sakurai, T.; Ohta, H.; Takahashi, K. The Impact of the Next-Nearest Neighbor Dispersion Interactions on Spin Crossover Transition Enthalpy Evidenced by Experimental and Computational Analyses of Neutral π-Extended Heteroleptic Fe(III) Complexes. *Inorg. Chem.* **2020**, *59*, 12295–12303.
(22) Dutta, S.; Basu, P.; Chakravorty, A. Mononuclear Manganese(IV) in Tridentate ONO Coordination. Synthesis, Structure, and Redox Regulation via Oxygen Donor Variation. *Inorg. Chem.* **1991**, *30*, 4031–4037.
(23) Moré, R.; Busse, G.; Hallmann, J.; Paulmann, C.; Scholz, M.; Techert, S. Photodimerization of Crystalline 9-Anthracenecarboxylic Acid: A Nontopotactic Autocatalytic Transformation. *J. Phys. Chem. C* **2010**, *114*, 4142–4148.
(24) Zöllner, H.; Woike, T.; Krasser, W.; Haussühl, S. Thermal Decay of Laser-Induced Long Living Metastable Electronic States in $Na_2[Fe(CN)_5NO] \cdot 2H_2O$ Single Crystals. *Z. für Krist.* **1989**, *188*, 139–153.
(25) Schaniel, D.; Woike, T.; Tsankov, L.; Imlau, M. Evidence of Four Light-Induced Metastable States in Iron-Nitrosyl Complexes. *Thermochim. Acta* **2005**, *429*, 19–23.
(26) Galli, S.; Mercandelli, P.; Sironi, A. Molecular Mechanics in Crystalline Media: The Case of (*E*)-Stilbenes. *J. Am. Chem. Soc.* **1999**, *121*, 3767–3772.
(27) Harada, J.; Ogawa, K. Pedal Motion in Crystals. *Chem. Soc. Rev.* **2009**, *38*, 2244–2252.
(28) Gaussian 16, Revision C.01, Frisch, M. J.; Trucks, G. W.; Schlegel, H. B.; Scuseria, G. E.; Robb, M. A.; Cheeseman, J. R.; Scalmani, G.; Barone, V.; Petersson, G. A.; Nakatsuji, H.; Li, X.; Caricato, M.; Marenich, A. V.; Bloino, J.; Janesko, B. G.; Gomperts, R.; Mennucci, B.; Hratchian, H. P.; Ortiz, J. V.; Izmaylov, A. F.; Sonnenberg, J. L.; Williams-Young, D.; Ding, F.; Lipparini, F.; Egidi, F.; Goings, J.; Peng, B.; Petrone, A.; Henderson, T.; Ranasinghe, D.; Zakrzewski, V. G.; Gao, J.; Rega, N.; Zheng, G.; Liang, W.; Hada, M.; Ehara, M.; Toyota, K.; Fukuda, R.; Hasegawa, J.; Ishida, M.; Nakajima, T.; Honda, Y.; Kitao, O.; Nakai, H.; Vreven, T.; Throssell, K.; Montgomery, J. A., Jr.; Peralta, J. E.; Ogliaro, F.; Bearpark, M. J.; Heyd, J. J.; Brothers, E. N.; Kudin, K. N.; Staroverov, V. N.; Keith, T. A.; Kobayashi, R.; Normand, J.; Raghavachari, K.; Rendell, A. P.; Burant, J. C.; Iyengar, S. S.; Tomasi, J.; Cossi, M.; Millam, J. M.; Klene, M.; Adamo, C.; Cammi, R.; Ochterski, J. W.; Martin, R. L.; Morokuma, K.; Farkas, O.; Foresman, J. B.; Fox, D. J. Gaussian, Inc., Wallingford CT, 2016.
(29) Salomon, O.; Reiher, M.; Hess, B. A. Assertion and Validation of the Performance of the B3LYP⋆ Functional for the First Transition Metal Row and the G2 Test Set. *J. Chem. Phys.* **2002**, *117*, 4729–4737.
(30) Peng, C.; Schlegel, H. B. Combining Synchronous Transit and Quasi-Newton Methods for Finding Transition States. *Israel J. Chem.* **1993**, *33*, 449–454.
(31) Henkelman, G.; Jonsson, H. Improved tangent estimate in the nudged elastic band method for finding minimum energy paths and saddle points. *J. Chem. Phys.* **2000**, *113*, 9978−9985.
(32) Nakajima, T.; Katouda, M.; Kamiya, M.; Nakatsuka, Y. NTChem: A high-performance software package for quantum molecular simulation. *Int. J. Quant. Chem.* **2015**, *115*, 349−359.
(33) Fukui, K. The Path of Chemical Reactions – The IRC Approach. *Acc. Chem. Res.* **1981**, *14*, 363–368.
(34) Rodríguez-Velamazán, J. A.; González, M. A.; Real, J. A.; Castro, M.; Muñoz, M. C.; Gaspar, A. B.; Ohtani, R.; Ohba, M.; Yoneda, K.; Hijikata, Y.; et al. A Switchable Molecular Rotator: Neutron Spectroscopy Study on a Polymeric Spin-Crossover Compound. *J. Am. Chem. Soc.* **2012**, *134*, 5083–5089.